OXFORD

Human Molecular Genetics, 2023, Vol. 32, 21, 3053–3062
https://doi.org/10.1093/hmg/ddad128
Advance access publication date 4 August 2023
Original Article

Lysyl oxidase-like 1-antisense 1 (*LOXL1-AS1*) lncRNA differentially regulates gene and protein expression, signaling and morphology of human ocular cells

Heather M. Schmitt[1,2], Kristyn M. Hake[1,2], Kristin M. Perkumas[1], Brandon M. Lê[2], Maria F. Suarez[1,2], Michael L. De Ieso[1], Rashad S. Rahman[1], William M. Johnson[1,2], María Gomez-Caraballo[1], Allison E. Ashley-Koch[2], Michael A. Hauser[1,2] and W. Daniel Stamer[1,*]

[1]Department of Ophthalmology, Duke University, Durham, NC 27710, USA
[2]Department of Medicine, Duke University, Durham, NC 27710, USA
*To whom correspondence should be addressed at: Duke Eye Center, 2351 Erwin Road, AERI Rm 4008, Durham, NC 27710, USA. Tel: 919-684-3745; Email: dan.stamer@duke.edu

Abstract

Pseudoexfoliation glaucoma (PEXG) is characterized by dysregulated extracellular matrix (ECM) homeostasis that disrupts conventional outflow function and increases intraocular pressure (IOP). Prolonged IOP elevation results in optic nerve head damage and vision loss. Uniquely, PEXG is a form of open angle glaucoma that has variable penetrance, is difficult to treat and does not respond well to common IOP-lowering pharmaceuticals. Therefore, understanding modulators of disease severity will aid in targeted therapies for PEXG. Genome-wide association studies have identified polymorphisms in the long non-coding RNA lysyl oxidase-like 1-antisense 1 (*LOXL1-AS1*) as a risk factor for PEXG. Risk alleles, oxidative stress and mechanical stretch all alter *LOXL1-AS1* expression. As a long non-coding RNA, *LOXL1-AS1* binds hnRNPL and regulates global gene expression. In this study, we focus on the role of *LOXL1-AS1* in the ocular cells (trabecular meshwork and Schlemm's canal) that regulate IOP. We show that selective knockdown of *LOXL1-AS1* leads to cell-type-specific changes in gene expression, ECM homeostasis, signaling and morphology. These results implicate *LOXL1-AS1* as a modulator of cellular homeostasis, altering cell contractility and ECM turnover, both of which are well-known contributors to PEXG. These findings support *LOXL1-AS1* as a key target for modifying the disease.

Introduction

Pseudoexfoliation glaucoma (PEXG) is an ocular manifestation of pseudoexfoliation syndrome (PEX), which is characterized by the accumulation of extracellular matrix (ECM) in the outflow pathway, leading to the dysregulation of conventional outflow and subsequent increase in intraocular pressure (IOP) (1–3). Increased IOP imparts mechanical injury to unmyelinated retinal ganglion cell axons at the optic nerve head, leading to apoptosis and subsequent loss of vision. Significantly, an estimated 50% of open angle glaucoma is caused by PEX (4). Interestingly, PEXG, like other types of primary open angle glaucoma (POAG), is an outflow pathway disease, but does not respond to front line IOP-lowering drugs as well as other forms of glaucoma (5,6). Aside from treatment difficulties, PEXG is affected by a complex set of genetic interactions and pathways (2,7,8). Moreover, PEXG is a genetically distinct form and understudied compared with other forms of glaucoma (9–11), potentially providing unique therapeutic opportunities.

Polymorphisms in the long non-coding RNA *LOXL1-AS1* are strongly associated with PEXG (7,12,13). *LOXL1-AS1* is upregulated in Schlemm's canal (SC) cells exposed to mechanical stretch and downregulated when exposed to oxidative stress in human lens epithelial (B3) cells, indicating a role for *LOXL1-AS1* in cellular environmental response pathways (13). Additionally, we have previously shown that *LOXL1-AS1* binds RNA-binding proteins, primarily the splicing protein hnRNPL, and regulates gene expression in immortalized human lens epithelial B3 cells (14). A pleiotropic genetic regulator such as *LOXL1-AS1* thus represents a valuable candidate for therapeutics in PEXG patients, who exhibit dysregulation of multiple genes, in pathways enriched for viral gene expression, mitochondrial and ribosomal respiratory transport and cell adhesion (15).

To better understand the complex role of *LOXL1-AS1* in PEXG, we examine the molecular landscape in PEXG-relevant cells. Specifically, we investigate whether depletion of *LOXL1-AS1* modulates gene expression in cells that regulate IOP using primary cultures of human trabecular meshwork (TM) and SC cells and then comparing results with gene expression studies in the transformed B3 cell line previously studied (14). This study also explores whether the loss of *LOXL1-AS1* expression affects downstream mechanotransduction signaling hub proteins, ECM proteins and cellular morphology, which are critical processes in the maintenance of conventional outflow function and IOP.

Results

LOXL1-AS1 regulates pleiotropic gene expression

LOXL1-AS1 regulates gene expression in models of cancer and ocular disease (14,16). In previous work, knockdown (KD) of

Received: February 28, 2023. **Revised:** June 19, 2023. **Accepted:** August 1, 2023

LOXL1-AS1 in B3 cells leads to dysregulation of over 450 RNAs, indicating that it is a major regulator of gene expression in this ocular cell type (14). To determine the gene targets of *LOXL1-AS1* in cells relevant to IOP regulation, RNA-seq analysis was performed on primary cultures of TM ($n = 7$ different strains) and SC ($n = 6$ different strains) cells transduced with Ad5-*LOXL1-AS1*-shRNA-GFP (*LOXL1-AS1* KD) or Ad5-Scrambled-shRNA-GFP (scrambled). Only cells that were confirmed to have a significant knockdown of *LOXL1-AS1* in comparison with control (>50%) were included in the study (Supplementary Material, Fig. S1). Compared with the 450 genes regulated in B3 cells (14), *LOXL1-AS1* knockdown significantly dysregulated only 220 gene targets in TM cells, and 24 in SC cells ($P < 0.05$) (Fig. 1A and B). These data, combined with previous results in B3 cells (14), demonstrate that *LOXL1-AS1* regulates gene expression in a cell-specific manner. The baseline levels of expression of a small number of (9) transcripts were present in TM cells but not SC cells, but a vast majority of transcripts were present at detectable basal levels in both cell types (data not shown).

LOXL1-AS1 regulates ECM gene expression

ECM dysregulation contributes to the pathology of PEXG (15,17,18). To focus on ECM targets using a second assay, we investigated the effect of *LOXL1-AS1* knockdown in TM, SC and B3 cells, using an ECM-based qPCR platform (Fig. 2). In primary TM cells ($n = 4$ different strains), knockdown of *LOXL1-AS1* led to significant dysregulation of gene targets such as collagen type XI, alpha 1 (*COL11A1*) and integrin beta 3 (*ITGB3*) ($^*P < 0.05$) (Fig. 2A), and western blot analysis revealed an upward trend in ITGB3 and a significant downregulation of COL11A1 protein ($^*P < 0.05$) (Fig. 2D). Knockdown of *LOXL1-AS1* in SC cells ($n = 4$ different strains) led to significant dysregulation of genes that included integrin alpha 2 (*ITGA2*) and laminin gamma 1 (*LAMC1*) ($^*P < 0.05$) (Fig. 2B), but no significant differences in protein levels were observed ($P > 0.05$) (Fig. 2E). In B3 cells, knockdown of *LOXL1-AS1* led to a significant upregulation of targets such as thrombospondin 2 (*THBS2*) and tenascin C (*TNC*) and downregulation of C-type lectin domain family 3, member B (*CLEC3B*) and TIMP metallopeptidase inhibitor-1 (*TIMP1*) ($^*P < 0.05$) (Fig. 2C). However, we observed no significant changes in protein abundance for TIMP1 and THBS2, ($P > 0.05$) (Fig. 2F). In summary, ECM targets respond in a cell-type-specific manner to knockdown of *LOXL1-AS1*. Interestingly, at the protein expression level, only downregulation of COL11A1 was significant in response to *LOXL1-AS1* knockdown in TM cells.

LOXL1-AS1 regulates mechanotransduction hub protein abundance and activity

Alterations in mechanotransduction protein expression occur in outflow pathway cells in response to mechanical stretch (19–21). In cancer cell lines, changes in *LOXL1-AS1* expression impact mechanotransduction hub protein expression, which leads to changes in cell proliferation, migration and morphology (22,23). Here, we investigate the protein expression profile and activity states for known mechanotransduction hub proteins: protein kinase B (AKT), focal adhesion kinase (FAK), mitogen-activated kinase (MAPK), yes-associated protein (YAP), tafazzin (TAZ), vertebrate lonesome kinase (VLK), Talin-1, Vinculin and RAS homolog family member A (RhoA) in response to *LOXL1-AS1* knockdown in human ocular cells. Surprisingly, we observed no change in any candidate hub proteins analyzed following *LOXL1-AS1* knockdown in TM cells (Fig. 3A). In contrast, AKT was robustly phosphorylated in SC cells following *LOXL1-AS1* knockdown (Fig. 3B). In B3 cells, knockdown of *LOXL1-AS1* led to significant phosphorylation of MAPK, dephosphorylation of AKT and downregulation of VLK, Talin-1 and RhoA ($^*P < 0.05$, $^{**}P < 0.01$, $^{***}P < 0.001$) (Fig. 3C). Interestingly, *LOXL1-AS1* knockdown reduced AKT phosphorylation in B3 cells while increasing it in TM and SC cells, indicating a cell-type-dependent role for this hub protein. YAP/TAZ was assessed by immunofluorescence microscopy and did not translocate to the nucleus, which indicated that the complex was not activated with *LOXL1-AS1* knockdown in the three cell types tested (data not shown).

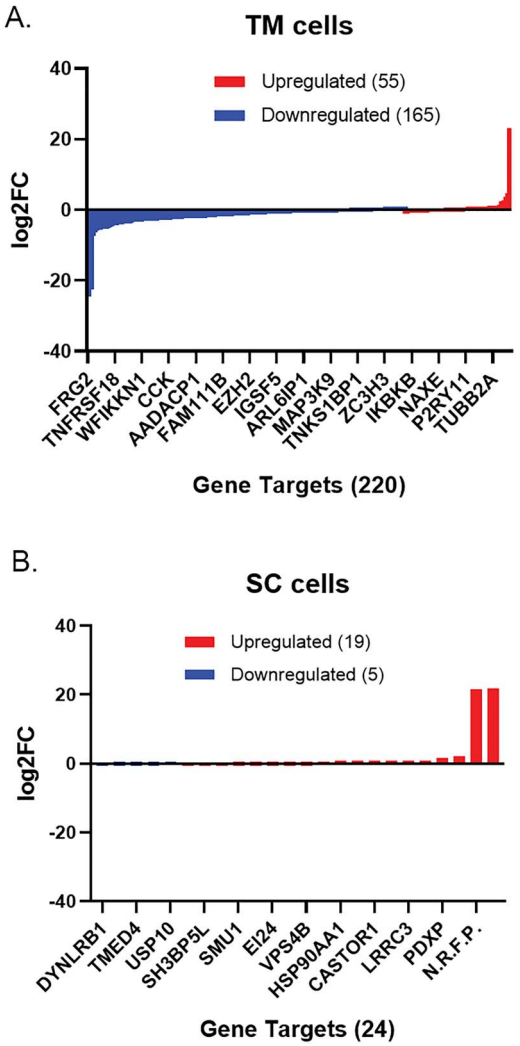

Figure 1. *LOXL1-AS1* knockdown differentially affects gene expression in TM and SC. Primary TM and SC cells were transduced with Ad5-Scrambled-shRNA-GFP (Scr) or Ad5-*LOXL1-AS1*-shRNA-GFP (KD) and analyzed at 72 h post-transduction for changes in global gene regulation. (**A**) In TM cells, there were 165 significantly downregulated and 55 significantly upregulated targets upon RNAseq analysis ($P < 0.05$), $n = 7$ cell strains. (**B**) In SC cells, there were only five significantly downregulated targets and 19 significantly upregulated targets upon RNAseq analysis ($P < 0.05$), $n = 6$ cell strains.

LOXL1-AS1 regulates cellular morphology

Lens and TM cells can undergo an endothelial to mesenchymal transition (EMT) in response to dysregulation of critical ECM pathway biomarkers (24–28). Moreover, *LOXL1-AS1* regulates proliferation, migration and EMT in cancer cells (22,29,30). Here,

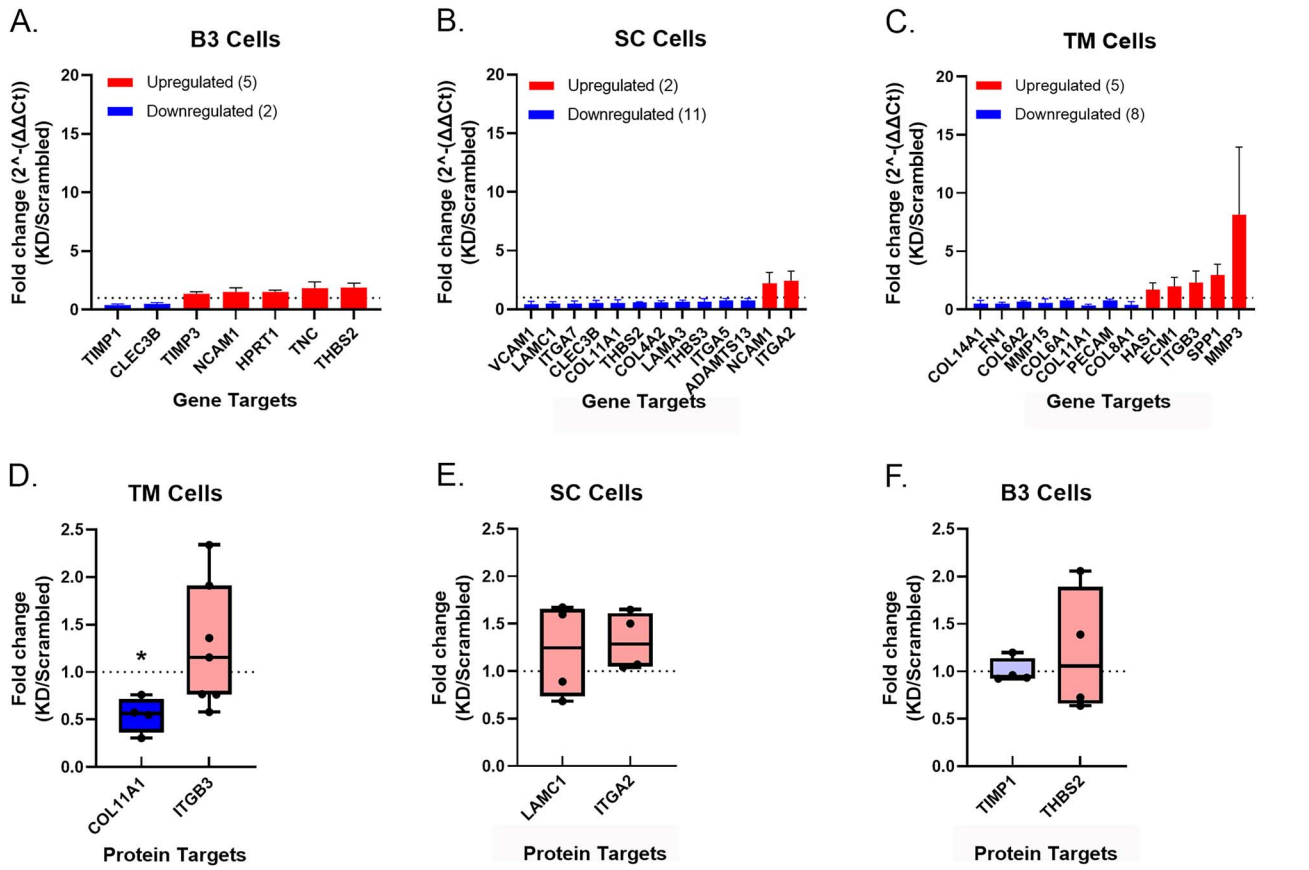

Figure 2. *LOXL1-AS1* knockdown differentially affects ECM target gene expression. Human immortalized lens epithelial (B3) cells, primary TM cells and primary SC cells underwent knockdown of *LOXL1-AS1* via transfection or transduction, respectively, and all cell types were analyzed specifically for ECM gene and protein expression. (**A**) In TM cells at 72 h post transduction, five gene targets were significantly upregulated, including Integrin beta-3 (*ITGB3*), and eight gene targets were significantly downregulated, including Collagen type XI, alpha 1 (*COL11A1*) ($P < 0.05$), $n = 4$ cell strains. (**B**) In SC cells at 72 h post transduction, two gene targets were significantly upregulated, including Integrin alpha-2 (*ITGA2*), and 11 gene targets were significantly downregulated, including Laminin gamma 1 (*LAMC1*) ($P < 0.05$), $n = 4$ cell strains. (**C**) In B3 cells at 48 h post transfection, five gene targets were significantly upregulated, including Thrombospondin-2 (*THBS2*), and two targets were significantly downregulated, including TIMP metallopeptidase inhibitor 1 (*TIMP1*) ($P < 0.05$), $n = 3$ biological replicates. (**D**) Western blot analysis performed on *LOXL1-AS1* knockdown TM cell lysates indicated that Collagen type IX, alpha 1 was significantly downregulated at the protein level ($P < 0.05$), $n = 4$ cell strains. ICAM-1 and Integrin beta3 were not significantly different at the protein level from scrambled controls ($P > 0.05$), $n = 7$ cell strains. (**E**) Upon western blot analysis on SC cell lysates for Laminin gamma 1 and Integrin alpha 2, no significant change was detectable at the protein level ($P > 0.05$), $n = 4$ cell strains. (**F**) Lastly, western blot analysis in B3 cell lysates for TIMP-1 and Thrombospondin-2 showed no significant change was detectable at the protein level in *LOXL1-AS1* knockdown cells ($P > 0.05$), $n = 4$ biological replicates.

we investigate whether knockdown of *LOXL1-AS1* affects ocular cell morphology. Three days after knockdown of *LOXL1-AS1*, TM cells trended toward circularity (Fig. 4A-C), but, significantly, SC cells displayed an EMT-like transition from elongated cell shapes to more circular cell shapes (***$P < 0.001$) (Fig. 4D–F). No change was observed as a result of *LOXL1-AS1* knockdown in B3 cells (Fig. 4G–I). To test whether the morphological change in SC cells was due to an increase in contractility, we measured the ratio of phosphorylated myosin light chain (MLC) to total MLC, a surrogate indicator of contractility (31–33). Protein analysis at 72 h post- *LOXL1-AS1* knockdown showed a trend toward a decrease in MLC activity ($P = 0.0563$) (Fig. 5). This decrease in MLC activity is consistent with morphological 'rounding' observed (Fig. 4).

Discussion

There are two common isoforms of *LOXL1-AS1*: one expressed in fibroblasts (ENST00000566011) and a second predominant form that is expressed in all other tissues (13,14). The predominant form of *LOXL1-AS1* is positioned within a locus associated with risk for PEXG. This isoform displays decreased expression in B3 cells with oxidative stress, shows increased expression in SC cells under mechanical stretch and regulates global gene expression in immortalized B3 cells (13,14). The data presented here extend these findings and show that the predominant form of *LOXL1-AS1* also regulates gene expression in primary TM and SC cells, although the number of target genes is reduced, and the identity of those targets is different. These genetic changes corresponded to alterations in ECM and mechanotransduction targets as well as cell shape changes in a cell-specific manner.

The activity for *LOXL1-AS1* in global gene regulation appears to be cell-type specific, yet the number of genes dysregulated decreases from B3 to TM to SC cells. This phenomenon could occur due to differences in cell strain source or cellular function in these tissues of the anterior segment. B3 cells were isolated from 18-week prenatal lenses (34) and were subsequently immortalized, making them genetically homogeneous. In contrast, primary cultures of TM and SC cells were isolated from different, mostly adult or elderly human donor eyes. This adds genetic variability between donors and possibly aging and environmentally induced epigenetic imprinting that can alter gene expression at baseline

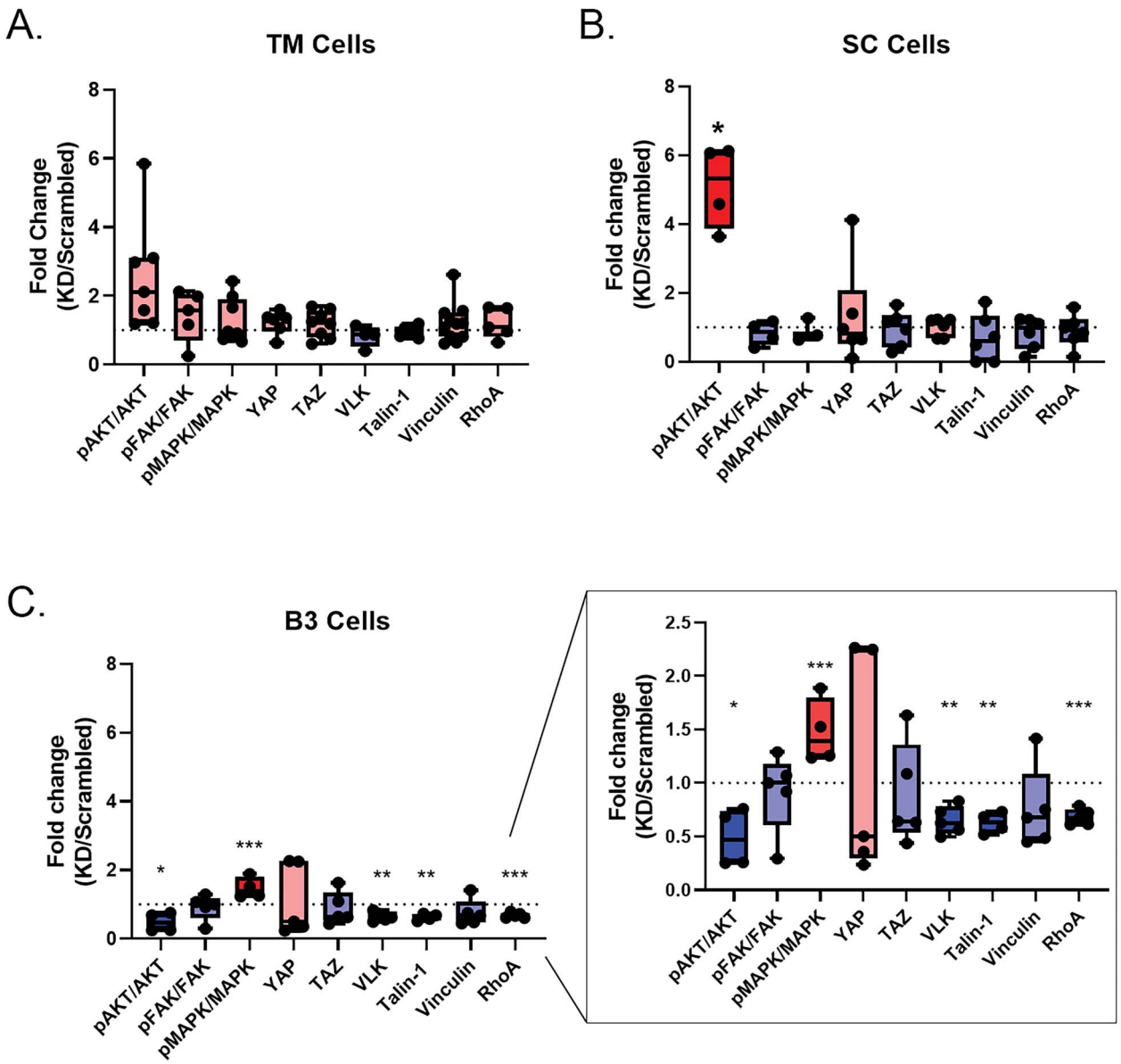

Figure 3. *LOXL1-AS1* knockdown differentially affects mechanotransduction targets in B3, TM and SC cells. Human primary TM cells, primary SC cells and immortalized lens cells (B3 cells) underwent knockdown of *LOXL1-AS1* via transduction or transfection, respectively, and all cell types were analyzed specifically for known mechanotransduction protein expression via western blot. (**A**) In TM cells at 72 h post transduction, no targets were significantly dysregulated with *LOXL1-AS1* knockdown ($P > 0.05$), $n = 3$–11 cell strains. (**B**) In SC cells at 72 h post transduction, pAKT/AKT was significantly upregulated ($P < 0.05$), $n = 4$ cell strains, while all other targets showed no significant change with *LOXL1-AS1* knockdown ($P > 0.05$), $n = 3$–6 cell strains. These data indicate differential mechanotransduction regulation for lens and outflow pathway cell types. (**C**) In B3 cells at 48 h post transfection, phosphorylated MAPK (pMAPK/MAPK) was upregulated, while pAKT/AKT, VLK, Talin-1 and RhoA were all significantly downregulated with *LOXL1-AS1* knockdown (*$P < 0.05$, **$P < 0.01$, ***$P < 0.001$), $n = 4$–5 biological replicates.

prior to *LOXL1-AS1* depletion in our experiments. However, this is unlikely to fully explain the differential gene targeting observed between the three ocular cell types. Each cell type is highly specialized, serving vastly different functions in the eye. Lens cells are epithelia, containing high concentrations of cytosolic proteins that function to refract incoming light (35). Conversely, TM cells are mesenchymal, which are phagocytic and contractile cells embedded in a complex avascular ECM architecture that serves as a biological filter and resistor system for aqueous humor (36). SC cells are enigmatic in their identity as a hybrid blood vascular/lymphatic cell type, responsible for maintaining part of the blood-aqueous barrier and regulating outflow of aqueous humor (37). Therefore, baseline abundance of messenger RNAs is expected to be different between the three cell types, as they serve vastly different roles in their physiological environment.

More important than numbers of dysregulated genes are the types of genes that are dysregulated in each cell type with depletion of *LOXL1-AS1*. For example, vasorin (VASN), a molecule responsible for binding transforming growth factor (TGF) and negatively regulating endothelial to mesenchymal transition (38), was downregulated in TM cells by RNAseq. In one previous study, VASN was significantly downregulated in primary TM cells from patients with POAG when compared with controls (38), possibly indicating an important role of *LOXL1-AS1* in regulating VASN-mediated TGF and EMT responses. In RNAseq data from SC cells, pyridoxal phosphate phosphatase (*PDXP*), a molecule that increases downstream endothelial permeability (39), was upregulated in response to *LOXL1-AS1* depletion. Aqueous outflow regulation is, in part, modulated by the permeability of SC's inner wall, making *LOXL1-AS1* a potentially critical regulator

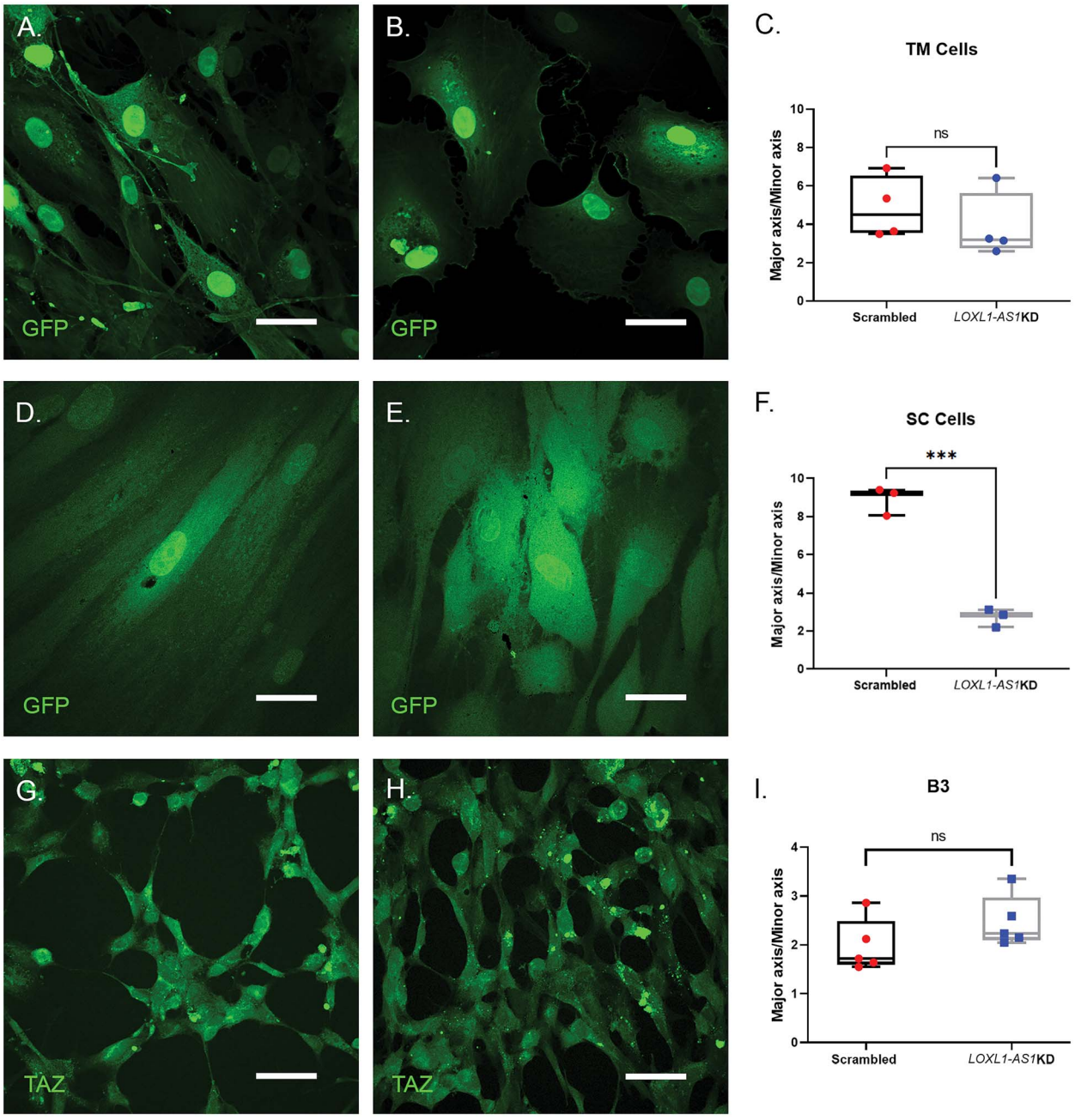

Figure 4. *LOXL1-AS1* knockdown changes B3, TM and SC morphology. Human primary TM cells, primary SC cells and immortalized lens epithelial (B3) cells underwent knockdown of *LOXL1-AS1* via viral transduction or plasmid transfection, respectively, and all cell types were analyzed specifically for cell morphology using immunofluorescence of either GFP or labeled TAZ with Al488 secondary antibody. (**A–C**) TM cells displayed a non-significant trend toward circularity between the Scrambled (**A**) and the *LOXL1-AS1* knockdown (**B**) cells, as indicated by (**C**) a decrease in semiaxis ratio (Major axis/Minor axis) ($P < 0.05$). Scale bar = 10 μm. (**D–F**) SC cells displayed a significant increase in circularity between the scrambled (**D**) and the *LOXL1-AS1* knockdown (**E**) cells, as indicated by (**F**) a decrease in semiaxis ratio (Major axis/Minor axis) ($P < 0.05$). Scale bar = 10 μm. (**G–I**) B3 cells displayed no change in circularity between the Scrambled (**A**) and the *LOXL1-AS1* knockdown (**B**) cells, as indicated by (**C**) a similar in semiaxis ratio (Major axis/Minor axis). Scale bar = 10 μm. Images were brightened equally to visualize cell borders.

of this process. This dysregulation of factors known to affect downstream signaling and conformational changes in outflow cell types led to our investigation into changes in expression of ECM targets, which are known to play a pivotal role in PEXG progression via maladaptive accumulation and induction of structural abnormalities both intercellularly and intracellularly.

ECM dysregulation and accumulation are diagnostic features of PEX (40,41), and this study elaborates on the role of *LOXL1-AS1* in regulating ECM targets in TM, SC and B3 cells. Dysregulated targets include basement membrane proteins, MMPs, cell adhesion molecules and signaling molecules. Although these targets were significantly dysregulated at the gene expression level, COL11A1 was significantly downregulated in TM cells at the protein level, indicating a potential breakdown in ECM fibrils, as COL11A1 is known to regulate fibril formation (42). COL11A1 is also downregulated in pathologies including fibrosis (43), where fibril size and length are abnormally heterogenous as a direct result of loss of COL11A1 expression. *LOXL1-AS1* may, therefore, play a role in regulating downstream fibrotic pathways that can contribute to PEXG progression through modulating ECM targets like COL11A1.

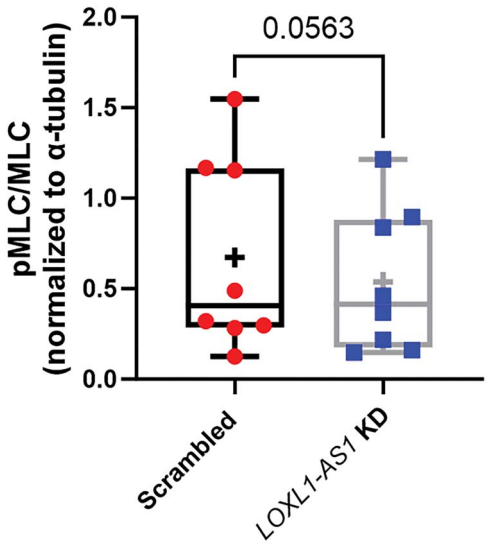

Figure 5. *LOXL1-AS1* knockdown decreases myosin light chain activity. Primary human SC cells were transduced with an adenoviral construct to knockdown *LOXL1-AS1*. 72 h post transduction cells were lysed and levels of phosphorylated MLC and total MLC were measured via western blotting. Results indicated a downward trend in pMLC/MLC following *LOXL1-AS1* knockdown, albeit not statistically significant ($P = 0.0563$), $n = 8$ biological replicates.

ECM fibrillary deposition is a major characteristic of PEXG in patients (37,38); however this phenomenon has not been observed in cell strains isolated from donor eyes of healthy patients *in vitro*. In contrast, ECM fibrillary deposits have been observed *ex vivo* in lens tissues from PEXG patients (44). More studies are needed to determine the effect of *LOXL1-AS1* depletion on ECM pathways and intermediate signaling molecule status.

Because we previously observed that *LOXL1-AS1* expression was upregulated with mechanical stretch in SC cells (13), we focused in this study on changes in hub signaling proteins that are responsive to mechanical stress (19–21,45) and important regulators of conventional outflow function. These hub proteins included pAKT/AKT, pMAPK/MAPK, pFAK/FAK, YAP, TAZ, VLK, talin-1, vinculin and rhoA. For example, phosphorylation of AKT is associated with a decrease in TM cell size (46) and an increase in phosphorylation of eNOS in SC cells (47), as well as signaling in processes such as proliferation, cell cycle and EMT responses (34,48). Activation of MAPK by phosphorylation regulates processes including proliferation, differentiation, motility and survival (49). In TM cells, MAPK is activated in response to mechanical stretch, and cells underwent cytoskeletal and morphologic changes (50). FAK is a protein tyrosine kinase that regulates cellular adhesion, motility, proliferation and survival in various types of cells (51). In TM cells, the phosphorylation status of FAK regulates the stability of actin cytoskeleton and cellular adhesions, therefore affecting cell shape *in vitro* and outflow facility *in vivo* (52). The activity of the YAP/TAZ axis is known to regulate stiffness in TM cells under TGFβ2 stress (53), and the activity of the RhoA/ROCK-YAP/TAZ axis regulates fibrosis in TM cells (54). VLK has been implicated in the processes of ECM protein phosphorylation, cell morphology and adhesion in TM cells (55). Talin-1 regulates communication between the actin cytoskeleton and the ECM (56), and it has been shown that cooperative $\alpha5\beta1/\alpha4\beta1$ integrin signaling affects talin localization and cytoskeletal organization in TM cells (57). Vinculin regulates linkage of talin to actin in the cytoskeleton and integrins in the cell membrane, thereby coupling changes in tension within the contractive cytoskeleton applied to the ECM (58).

After *LOXL1-AS1* KD in ocular cells, we discovered that TM, SC and B3 cell responses varied. For instance, phosphorylated AKT/-total AKT was significantly downregulated in B3 cells, upregulated in SC cells and trending toward upregulated in TM cells. This, coupled with the significant activation of MAPK, deactivation of AKT and downregulation of VLK and Talin-1 in B3 cells, indicates a very different mechanotransduction response in primary outflow cells compared with immortalized lens cells. Since part of the PEXG characteristic ECM deposition is thought to originate in lens cells (41), these data corroborate previous studies displaying the dysregulation of a group of mechanotransduction pathways that likely regulate this process in ocular cell types (38,59–61). However, the physiological response to *LOXL1-AS1* depletion was more robust in TM and SC cells via AKT activation, leading to a potential pathway for ECM remodeling in the outflow cell types that may regulate cell morphology and physiological function.

To withstand the extreme mechanical forces in the conventional outflow pathway, TM and SC cells are highly contractile, similar to smooth muscle cells (62,63). However, fibrosis can be a pathological consequence of abnormal responses of cells to mechanical stress. Interestingly, we observed complementary indications that *LOXL1-AS1* mediates contractile tone of both TM and SC cells, either indirectly via changes in its ECM expression or directly affecting their contractile machinery. As such we observed that knockdown of *LOXL1-AS1* affected the morphology of both outflow cell types, significantly rounding SC cells (Fig. 4). When looking closer at the contractile machinery in SC cells we observed a decrease in MLC phosphorylation after *LOXL1-AS1* knockdown, nearly reaching statistically significant levels (Fig. 5). Such effects are reminiscent of the rounded morphology and reduced contractile tone reported in TM and SC after treatment with rho kinase inhibitors that directly block MLC phosphorylation and increases outflow facility (64–68). Future studies will be directed at examining the effect of *LOXL1-AS1* knockdown on outflow facility in perfused human anterior segments.

The gene expression profiles, signaling molecule activity and morphological changes associated with *LOXL1-AS1* depletion in TM, SC and B3 cells in this study provide key information to support further investigation into the dynamic role of this lncRNA, as it applies to PEXG. This investigation shows that *LOXL-AS1* regulates pleiotropic and ECM-specific gene expression profiles in a cell-type-dependent manner and that outflow pathway cell-specific regulation of AKT may mitigate cellular morphology changes downstream. These findings are critical to understanding how *LOXL1-AS1* imparts risk for PEXG and how this lncRNA may directly regulate outflow cell ECM and morphological changes. Future studies into the physiological significance of *LOXL1-AS1* dysregulation in *ex vivo* tissues may provide further insight into the downstream effects of *LOXL1-AS1*-mediated cell signaling and morphology changes on aqueous outflow dynamics. In conclusion, *LOXL1-AS1* is an important and dynamic regulator in ocular cells and requires further investigation to determine optimal therapeutic targeting for PEXG.

Materials and Methods

Cell culture

Immortalized human lens epithelial HLE-B3 (B3) cells (#CRK-11421, ATCC, Manassas, VA) were cultured in high glucose Dulbecco's modified Eagle's medium (DMEM) (+) sodium pyruvate, (+) glutamine (#11965092, Thermo Fisher Scientific, Raleigh, NC), and supplemented with 20% fetal bovine serum (FBS) (#11550, Atlanta Biologicals, Flowery Branch, GA), 1X PSG

(#10378016, Thermo Fisher Scientific) and 55 mg/L of non-essential amino acids (#11140–050, Thermo Fisher Scientific).

Ocular tissues were harvested from male and female donors without diagnosed ocular disease, minimizing to the best of our ability the underlying genetic effects that could alter the downstream regulatory outcomes with *LOXL1-AS1* manipulation. TM cells were isolated from human donor eyes using an ECM digestion protocol as previously described (69). TM cells were characterized by cellular morphology, contact inhibition and robust induction of myocilin protein following treatment with 100 nM of dexamethasone over 5 days (70). Cells were confirmed to be TM by immunofluorescence microscopy and western blot analysis. TM cells were cultured in low glucose DMEM (#11885092, Thermo Fisher Scientific) and supplemented with 1% PSG and 10% FBS.

SC were isolated from human donor eyes using a previously established protocol (71). Briefly, cadaveric anterior chambers were dissected into eight equal and radially symmetric pieces, a gelatin-coated suture was cannulated through the lumen of the SC and cannulated pieces were cultured for 3 weeks. Sutures were then removed from the SC, and cells were seeded onto 3 cm culture plates. SC cells were then characterized by morphology, growth characteristics and cell-specific markers (72). SC cells were cultured with DMEM, 10% FBS and 1% PSG.

TM, SC and B3 cells were incubated at 37°C, 5% CO2 and grown to 80–90% (60–70% for B3 cells) confluency prior to *LOXL1-AS1* knockdown studies.

LOXL1-AS1 knockdown

B3 cells were grown to 60–70% confluency in a 6-well plate, then transfected with lipofectamine RNAiMAX (#13778075) in Opti-MEM media (#31985062), and a *LOXL1-AS1* targeted small interfering RNA (siRNA) (target sequence: 5′- CACAGAAGAGGT-GCTCGATAA-3′ in the last exon conserved in both splice forms of *LOXL1-AS1*) (#S105724243) or a negative control scramble siRNA (#S103650318) (Qiagen, Germantown, MD). At 6 h post transfection, an additional 1 ml of B3 media was overlaid. At 48 h post-transfection, B3 cells were rinsed in cold phosphate-buffered saline (PBS) and harvested.

Viral titer experiments were performed in both TM and SC cells to determine the lowest multiplicity of infection (MOI) to effectively knock down *LOXL1-AS1*. At 80% confluency, TM cells were transduced with an MOI of 10 with adenovirus containing either a short hairpin RNA (shRNA) targeted to *LOXL1-AS1* (target sequence: 5′- CACAGAAGAGGTGCTCGATAA-3′ in the last exon conserved in both splice forms of *LOXL1-AS1*) with a GFP reporter or a negative control scrambled shRNA with a GFP reporter for 6 h before adding 1 ml of media. After 72 h, cells were rinsed in PBS and harvested.

LOXL1-AS1 was knocked down in SC cells at 80% confluency by transduction with Ad5.*LOXL1-AS1*shRNA.GFP at an MOI of 200 or using lipofectamine RNAiMAX to transfect Ad5.*LOXL1-AS1*shRNA.GFP at an MOI of 10 into the cells. Ad5.*Scrambled*.GFP transduction was used as a control. Lipofectamine combined with adenovirus was determined to be more efficient than standard transduction techniques and permitted us to reduce the MOI to 10. At 72 h post-transfection, SC cells were rinsed in PBS and harvested. Knockdown was determined by qPCR from RNA isolated from each cell type.

RNA isolation and cDNA synthesis

Cells were mechanically lysed using Qiashredders (Qiagen, #79654), then RNA isolation was accomplished using the cell lysate in the Quick-RNA MiniPrep Kit (#11-327, Zymo Research) for TM, SC and B3 cells using the manufacturer's protocol. After isolating RNA, Template cDNA was generated using 1 μg of isolated RNA per sample. cDNA was generated using High-Capacity cDNA Reverse Transcription Kit (#4368814, Applied Biosystems).

RNAseq

RNAseq raw read data were analyzed to determine if any genes were differentially expressed in TM and SC cells after *LOXL1-AS1* knockdown. FastQC (https://www.bioinformatics.babraham.ac.uk/projects/fastqc/) was used to assess read quality. Trim Galore (https://www.bioinformatics.babraham.ac.uk/projects/trim_galore/) was used to trim read adapters and filter out reads with a Phred score of <20. SALMON (73) was used to quantify expression levels of the reads using its mapping-based mode. A transcriptome index was generated using the Ensembl 106 release of the GRCh38 *homo sapiens* cDNA transcripts, and quantification was performed with the sequence-specific bias and GC bias corrections. The resulting quantifications were then used in DESeq2 (74) to perform the differential gene expression analyses across TM cells, SC cells and TM and SC cells combined.

Quantitative PCR

To confirm *LOXL1-AS1* knockdown, quantitative PCR was performed using TaqMan Fast Advanced Master Mix (#4444557, Thermo Fisher Scientific), Taqman assays (#Hs00173746: *LOXL1-AS1* and #Hs02758991: GAPDH, Thermo Fisher Scientific) and the QuantStudio3 (Applied BioSystems, Waltham, MA) as per manufacturer protocol. For the ECM assay, 96-well plates (pahs-013zd, Qiagen) preloaded with various ECM targets were used in conjunction with Qiagen RT^2 First Strand Kit and RT^2 SYBR Green qPCR Mastermix.

Protein isolation

Harvested cell pellets from TM, SC and B3 cells were resuspended in 50 μl RIPA buffer (#89900, Thermo Fisher Scientific) and 1 μl protease inhibitor (#P8340, Sigma Aldrich, St. Louis, MO). Samples were placed on ice for 45 min and vortexed every 5 min. Samples were spun at 14 000 RPM for 10 min to pellet cell debris, and supernatant was transferred to a new tube. Sample protein concentration was measured using Pierce BCA Protein Assay Kit (#23227, Thermo Fisher Scientific) and Molecular Devices SpectraMax M5 plate reader (Molecular Devices, San Jose, CA). Alternatively, for pMLC/MLC experiments, plates were immediately placed on ice at 72 h post viral transduction, and cells were rinsed three times with ice-cold PBS and harvested by scraping into 1X Laemmli sample buffer with 100 mM DL-dithiothreitol (#D9779, Sigma-Aldrich) at 200 μl/well. Protein lysates were boiled for 5 min and stored at −80°C.

Western blot analysis

A working sample buffer was made to prepare protein samples; 80 μl 2x Sample Buffer made from 4x Laemmli Sample Buffer (#1610747, Bio-Rad Laboratories, Hercules, CA), 20 μl beta-mercaptoethanol (#M6250-10ML, Sigma Aldrich, St. Louis, MO) and 50ul urea (# U4883, Sigma-Aldrich). The working sample buffer was added to protein samples 1:1 and incubated at room temperature for 10 min. Samples of 5–10ug were loaded on 10% SDS gels. Gels were transferred to membranes using the wet transfer method at 100 V for 1 h, followed by blocking for an hour in TBST +5% BSA, then overnight incubation of primary antibodies at 4°C. Primary antibodies include COL11A1 (#72026 T), ITGB3 (#13166), pAKT (S473) (# 4060 T), AKT (#4961S), pFAK(Y397)

(#8556 T), FAK (#3285S), pMAPK (phosphor-p44/42, T202/Y204) (#9101S), MAPK (#9271S), YAP (#8418S), TAZ (#8418S), Talin-1 (# 4021 T), Vinculin (#13901S), RhoA (#2117S), phospho-MLC (#3674), and MLC (#3672) (Cell Signaling, Danvers, MA); LAMC1 (#mab1920) and ITAG2 (#ab1936) (MilliporeSigma, Burlington, MA); TIMP1 (#IM32L, Oncogene Research Projects, La Jolla, CA); and THBS2 (#PA5-97117) and VLK (#PA5-30893) (Thermo Fisher Scientific). Membranes were washed in TBST three times before incubating in goat anti-rabbit HRP secondary antibody (#111-035-149, Jackson ImmunoResearch, West Grove, PA) or mouse monoclonal anti-alpha-tubulin HRP conjugate (#12351, Cell Signaling) for an hour and washing again. Membranes were developed with ECL-select (#Rpn2235) or ECL-prime (#Rpn2232) (Cytiva, Marlborough, MA). Membranes were imaged using BioRad's ChemiDoc Touch Imaging System. Blots were cropped and sized in Adobe Photoshop.

Immunofluorescence microscopy

At 72 h post-transduction for TM and SC cells or 48 h for B3 cells, the cells were rinsed with PBS and then fixed with chilled 4% paraformaldehyde (PFA) for 20 min at room temperature. B3 cells were then blocked in 5% BSA, and supplemented with 10% goat serum in TBST. Cells were then incubated in TAZ (#8418S, Cell Signaling) primary antibody overnight at 4°C. Cells were rinsed in TBST before incubating in goat anti-rabbit Al488 secondary antibody (#111-545-003, Jackson ImmunoResearch), for an hour at room temperature. Cells were rinsed again before finally adding DAPI (#D9542-1MG, Sigma Aldrich) and mounting coverslips to slides using Immu-mount (#9990412, Thermo Fisher Scientific). Cells were imaged at 40X magnification using Nikon AX Confocal microscope. ImageJ was used to analyze morphology of cells for semiaxis ratios. Images were brightened equally to visualize cell borders in Adobe Photoshop. Morphology data were obtained from the following replicates: B3 cells (25 cells/data point), TM cells (12–30 cells/data point; 4 cell strains) and SC cells (19–35 cells/data point; 3 cell strains).

Statistics

The sample size of each experiment is displayed in the figures or in the corresponding figure legends. To account for eye donor variability, we used a minimum of three different strains for SC and TM cells for each experimental set. The investigators were not masked to the study groups. In DESeq2, statistical significance was set at $P < 0.05$ using the Wald test and adjusted for false discovery with the Benjamini–Hochberg procedure. RNAseq graphs and ECM target graphs were generated with a significance cutoff of $P < 0.05$. Statistical significance was determined using paired and unpaired (with Welch's correction) t-test for protein and RNA expression. A paired Student t-test was used to determine significance for morphological changes based on semiaxis ratios. Alpha was set to 0.05.

Supplementary Material

Supplementary Material is available at *HMG* online.

Acknowledgements

We thank the Duke University School of Medicine core research facilities for confocal microscopy, Miracles in Sight Eye Bank and the Duke BioSight for ocular cell strain sources.

Conflict of Interest statement. The authors declare no conflict of interest.

Data availability

RNA sequencing and qPCR array data are available from corresponding author upon reasonable request.

Funding

Fight for Sight (to W.M.J.); Research to Prevent Blindness (to W.D.S., R.R.A., M.A.H.); LC Industries (to W.D.S., R.R.A., M.A.H.); The Glaucoma Foundation (to W.D.S., R.R.A.); and National Institutes of Health (R01EY028608 to M.A.H., R01EY022359 to W.D.S., R01EY030617 to W.D.S., M.A.H., P30EY005722 to W.D.S., R.R.A., M.A.H.).

References

1. Aboobakar, I.F., Johnson, W.M., Stamer, W.D., Hauser, M.A. and Allingham, R.R. (2017) Major review, exfoliation syndrome, advances in disease genetics, molecular biology, and epidemiology. *Exp. Eye Res.*, **154**, 88–103.
2. Johnson, W.M., Finnegan, L.K., Hauser, M.A. and Stamer, W.D. (2018) lncRNAs, DNA methylation, and the pathobiology of exfoliation glaucoma. *J. Glaucoma*, **27**, 202–209.
3. Schlotzer-Schrehardt, U. (2009) Molecular pathology of pseudoexfoliation syndrome/glaucoma – new insights from LOXL1 gene associations. *Exp. Eye Res.*, **88**, 776–785.
4. Ou, Y. (2021) Pseudoexfoliation (PEX) syndrome and Pseudoexfoliation glaucoma. *BrightFocus Foundation*, in press.
5. Lee, D.A. and Higginbotham, E.J. (2005) Glaucoma and its treatment: a review. *Am. J. Health Syst. Pharm.*, **62**, 691–699.
6. Wang, Z., Wiggs, J.L., Aung, T., Khawaja, A.P. and Khor, C.C. (2022) The genetic basis for adult onset glaucoma, recent advances and future directions. *Prog. Retin. Eye Res.*, **90**, 101066.
7. Aung, T., Ozaki, M., Lee, M.C., Schlotzer-Schrehardt, U., Thorleifsson, G., Mizoguchi, T., Igo, R.P., Jr., Haripriya, A., Williams, S.E., Astakhov, Y.S. *et al.* (2017) Genetic association study of exfoliation syndrome identifies a protective rare variant at LOXL1 and five new susceptibility loci. *Nat. Genet.*, **49**, 993–1004.
8. Thorleifsson, G., Magnusson, K.P., Sulem, P., Walters, G.B., Gudbjartsson, D.F., Stefansson, H., Jonsson, T., Jonasdottir, A., Jonasdottir, A., Stefansdottir, G. *et al.* (2007) Common sequence variants in the LOXL1 gene confer susceptibility to exfoliation glaucoma. *Science*, **317**, 1397–1400.
9. Chakraborty, M., Sahay, P. and Rao, A. (2021) Primary human trabecular meshwork model for Pseudoexfoliation. *Cell*, **10**, 3448.
10. Rao, K.N., Ritch, R., Dorairaj, S.K., Kaur, I., Liebmann, J.M., Thomas, R. and Chakrabarti, S. (2008) Exfoliation syndrome and exfoliation glaucoma-associated LOXL1 variations are not involved in pigment dispersion syndrome and pigmentary glaucoma. *Mol. Vis.*, **14**, 1254–1262.
11. Wolf, C., Gramer, E., Muller-Myhsok, B., Pasutto, F., Gramer, G., Wissinger, B. and Weisschuh, N. (2010) Lysyl oxidase-like 1 gene polymorphisms in German patients with normal tension glaucoma, pigmentary glaucoma and exfoliation glaucoma. *J. Glaucoma*, PMLR, Vienna, Austria, **19**, 136–141.
12. Challa, P., Schmidt, S., Liu, Y., Qin, X., Vann, R.R., Gonzalez, P., Allingham, R.R. and Hauser, M.A. (2008) Analysis of LOXL1 polymorphisms in a United States population with pseudoexfoliation glaucoma. *Mol. Vis.*, **14**, 146–149.
13. Hauser, M.A., Aboobakar, I.F., Liu, Y., Miura, S., Whigham, B.T., Challa, P., Wheeler, J., Williams, A., Santiago-Turla, C., Qin, X. *et al.* (2015) Genetic variants and cellular stressors associated with exfoliation syndrome modulate promoter activity of a lncRNA within the LOXL1 locus. *Hum. Mol. Genet.*, **24**, 6552–6563.

14. Schmitt, H.M., Johnson, W.M., Aboobakar, I.F., Strickland, S., Gomez-Caraballo, M., Parker, M., Finnegan, L., Corcoran, D.L., Skiba, N.P., Allingham, R.R., Hauser, M.A. and Stamer, W.D. (2020) Identification and activity of the functional complex between hnRNPL and the pseudoexfoliation syndrome-associated lncRNA, LOXL1-AS1. *Hum. Mol. Genet.*, **29**, 1986–1995.
15. Mullany, S., Marshall, H., Zhou, T., Thomson, D., Schmidt, J.M., Qassim, A., Knight, L.S.W., Hollitt, G., Berry, E.C., Nguyen, T. *et al.* (2022) RNA sequencing of lens capsular epithelium implicates novel pathways in Pseudoexfoliation syndrome. *Invest. Ophthalmol. Vis. Sci.*, **63**, 26.
16. Li, H., Chu, J., Jia, J., Sheng, J., Zhao, X., Xing, Y. and He, F. (2021) LncRNA LOXL1-AS1 promotes esophageal squamous cell carcinoma progression by targeting DESC1. *J. Cancer*, **12**, 530–538.
17. Ho, S.L., Dogar, G.F., Wang, J., Crean, J., Wu, Q.D., Oliver, N., Weitz, S., Murray, A., Cleary, P.E. and O'Brien, C. (2005) Elevated aqueous humour tissue inhibitor of matrix metalloproteinase-1 and connective tissue growth factor in pseudoexfoliation syndrome. *Br. J. Ophthalmol.*, **89**, 169–173.
18. Sahay, P., Reddy, S., Prusty, B.K., Modak, R. and Rao, A. (2021) TGF-beta1, MMPs and cytokines profiles in ocular surface, possible tear biomarkers for pseudoexfoliation. *PLoS One*, **16**, e0249759.
19. De Ieso, M.L., Kuhn, M., Bernatchez, P., Elliott, M.H. and Stamer, W.D. (2022) A role of Caveolae in trabecular meshwork Mechanosensing and contractile tone. *Front. Cell Dev. Biol.*, **10**, 855097.
20. Lakk, M. and Krizaj, D. (2021) TRPV4-rho signaling drives cytoskeletal and focal adhesion remodeling in trabecular meshwork cells. *Am. J. Phys. Cell Phys.*, **320**, C1013–C1030.
21. Shim, M.S., Nettesheim, A., Dixon, A. and Liton, P.B. (2021) Primary cilia and the reciprocal activation of AKT and SMAD2/3 regulate stretch-induced autophagy in trabecular meshwork cells. *Proc. Natl. Acad. Sci. U.S.A.*, **118**, e2021942118.
22. Gao, R., Zhang, R., Zhang, C., Liang, Y. and Tang, W. (2018) LncRNA LOXL1-AS1 promotes the proliferation and metastasis of Medulloblastoma by activating the PI3K/AKT pathway. *Anal. Cell. Pathol. (Amst.)*, **2018**, 9275685.
23. Zhang, P., Zhao, F., Jia, K. and Liu, X. (2022) The LOXL1 antisense RNA 1 (LOXL1-AS1)/microRNA-423-5p (miR-423-5p)/ectodermal-neural cortex 1 (ENC1) axis promotes cervical cancer through the mitogen-activated protein kinase (MEK)/extracellular signal-regulated kinase (ERK) pathway. *Bioengineered*, **13**, 2567–2584.
24. Chakrabarti, S., Kaur, K., Rao, K.N., Mandal, A.K., Kaur, I., Parikh, R.S. and Thomas, R. (2009) The transcription factor gene FOXC1 exhibits a limited role in primary congenital glaucoma. *Invest. Ophthalmol. Vis. Sci.*, **50**, 75–83.
25. Huang, P., Hu, Y. and Duan, Y. (2022) TGF-beta2-induced circ-PRDM5 regulates migration, invasion, and EMT through the miR-92b-3p/COL1A2 pathway in human lens epithelial cells. *J. Mol. Histol.*, **53**, 309–320.
26. Mastromonaco, C., Balazsi, M., Coblentz, J., Dias, A.B.T., Zoroquiain, P. and Burnier, M.N., Jr. (2022) Histopathological analysis of residual lens cells in capsular opacities after cataract surgery using objective software. *Indian J. Ophthalmol.*, **70**, 1617–1625.
27. Takahashi, E., Inoue, T., Fujimoto, T., Kojima, S. and Tanihara, H. (2014) Epithelial mesenchymal transition-like phenomenon in trabecular meshwork cells. *Exp. Eye Res.*, **118**, 72–79.
28. Kelly, R.A., Perkumas, K.M., Campbell, M., Farrar, G.J., Stamer, W.D., Humphries, P., O'Callaghan, J. and O'Brien, C.J. (2021) Fibrotic changes to Schlemm's canal endothelial cells in glaucoma. *Int. J. Mol. Sci.*, **22**, 9446.
29. Sun, Q., Li, J., Li, F., Li, H., Bei, S., Zhang, X. and Feng, L. (2019) LncRNA LOXL1-AS1 facilitates the tumorigenesis and stemness of gastric carcinoma via regulation of miR-708-5p/USF1 pathway. *Cell Prolif.*, **52**, e12687.
30. Yu, W. and Dai, Y. (2021) lncRNA LOXL1-AS1 promotes liver cancer cell proliferation and migration by regulating the miR-377-3p/NFIB axis. *Oncol. Lett.*, **22**, 624.
31. Kaneko-Kawano, T., Takasu, F., Naoki, H., Sakumura, Y., Ishii, S., Ueba, T., Eiyama, A., Okada, A., Kawano, Y. and Suzuki, K. (2012) Dynamic regulation of myosin light chain phosphorylation by rho-kinase. *PLoS One*, **7**, e39269.
32. Kimura, K., Ito, M., Amano, M., Chihara, K., Fukata, Y., Nakafuku, M., Yamamori, B., Feng, J., Nakano, T., Okawa, K., Iwamatsu, A. and Kaibuchi, K. (1996) Regulation of myosin phosphatase by rho and rho-associated kinase (rho-kinase). *Science*, **273**, 245–248.
33. Kureishi, Y., Kobayashi, S., Amano, M., Kimura, K., Kanaide, H., Nakano, T., Kaibuchi, K. and Ito, M. (1997) Rho-associated kinase directly induces smooth muscle contraction through myosin light chain phosphorylation. *J. Biol. Chem.*, **272**, 12257–12260.
34. Blakely, E.A., Bjornstad, K.A., Chang, P.Y., McNamara, M.P., Chang, E., Aragon, G., Lin, S.P., Lui, G. and Polansky, J.R. (2000) Growth and differentiation of human lens epithelial cells in vitro on matrix. *Invest. Ophthalmol. Vis. Sci.*, **41**, 3898–3907.
35. Wride, M.A. (2011) Lens fibre cell differentiation and organelle loss: many paths lead to clarity. *Philos. Trans. R. Soc. Lond. Ser. B Biol. Sci.*, **366**, 1219–1233.
36. Stamer, W.D. and Clark, A.F. (2017) The many faces of the trabecular meshwork cell. *Exp. Eye Res.*, **158**, 112–123.
37. Patel, G., Fury, W., Yang, H., Gomez-Caraballo, M., Bai, Y., Yang, T., Adler, C., Wei, Y., Ni, M., Schmitt, H. *et al.* (2020) Molecular taxonomy of human ocular outflow tissues defined by single-cell transcriptomics. *Proc. Natl. Acad. Sci. U. S. A.*, **117**, 12856–12867.
38. Choi, J.A., Maddala, R., Karnam, S., Skiba, N.P., Vann, R., Challa, P. and Rao, P.V. (2022) Role of vasorin, an anti-apoptotic, anti-TGF-beta and hypoxia-induced glycoprotein in the trabecular meshwork cells and glaucoma. *J. Cell. Mol. Med.*, **26**, 2063–2075.
39. Barabutis, N., Dimitropoulou, C., Gregory, B. and Catravas, J.D. (2018) Wild-type p53 enhances endothelial barrier function by mediating RAC1 signalling and RhoA inhibition. *J. Cell. Mol. Med.*, **22**, 1792–1804.
40. Rao, A. and Padhy, D. (2014) Pattern of Pseudoexfoliation deposits on the lens and their clinical correlation- clinical study and review of literature. *PLoS One*, **9**, e113329.
41. Sahay, P., Chakraborty, M. and Rao, A. (2022) Global and comparative proteome signatures in the lens capsule, trabecular meshwork, and iris of patients with Pseudoexfoliation glaucoma. *Front. Mol. Biosci.*, **9**, 877250.
42. Sun, M., Luo, E.Y., Adams, S.M., Adams, T., Ye, Y., Shetye, S.S., Soslowsky, L.J. and Birk, D.E. (2020) Collagen XI regulates the acquisition of collagen fibril structure, organization and functional properties in tendon. *Matrix Biol.*, **94**, 77–94.
43. Sun, M., Cogswell, D., Adams, S., Ayoubi, Y., Kumar, A., Reljic, T., Avila, M.Y., Margo, C.E. and Espana, E.M. (2022) Downregulation of collagen XI during late postnatal corneal development is followed by upregulation after injury. *J. Cell Sci.*, **135**, jcs258694.
44. De Maria, A., Zientek, K.D., David, L.L., Wilmarth, P.A., Bhorade, A.M., Harocopos, G.J., Huang, A.J.W., Hong, A.R., Siegfried, C.J., Tsai, L.M. *et al.* (2021) Compositional analysis of extracellular aggregates in the eyes of patients with exfoliation syndrome and exfoliation glaucoma. *Invest. Ophthalmol. Vis. Sci.*, **62**, 27.
45. McDonnell, F., Perkumas, K.M., Ashpole, N.E., Kalnitsky, J., Sherwood, J.M., Overby, D.R. and Stamer, W.D. (2020) Shear stress in

Schlemm's canal as a sensor of intraocular pressure. *Sci. Rep.*, **10**, 5804.
46. Xu, D., Wu, F., Yu, Y., Lou, X., Ye, M., Zhang, H. and Zhao, Y. (2022) Sympathetic activation leads to Schlemm's canal expansion via increasing vasoactive intestinal polypeptide secretion from trabecular meshwork. *Exp. Eye Res.*, **224**, 109235.
47. Lei, Y., Stamer, W.D., Wu, J. and Sun, X. (2014) Endothelial nitric oxide synthase-related mechanotransduction changes in aged porcine angular aqueous plexus cells. *Invest. Ophthalmol. Vis. Sci.*, **55**, 8402–8408.
48. Wang, Y., Chang, T., Wu, T., Ye, W., Wang, Y., Dou, G., Du, H., Hui, Y. and Guo, C. (2021) Connective tissue growth factor promotes retinal pigment epithelium mesenchymal transition via the PI3K/AKT signaling pathway. *Mol. Med. Rep.*, **23**, 389.
49. Cargnello, M. and Roux, P.P. (2011) Activation and function of the MAPKs and their substrates, the MAPK-activated protein kinases. *Microbiol. Mol. Biol. Rev.*, **75**, 50–83.
50. Tumminia, S.J., Mitton, K.P., Arora, J., Zelenka, P., Epstein, D.L. and Russell, P. (1998) Mechanical stretch alters the actin cytoskeletal network and signal transduction in human trabecular meshwork cells. *Invest. Ophthalmol. Vis. Sci.*, **39**, 1361–1371.
51. Yoon, H., Dehart, J.P., Murphy, J.M. and Lim, S.T. (2015) Understanding the roles of FAK in cancer, inhibitors, genetic models, and new insights. *J. Histochem. Cytochem.*, **63**, 114–128.
52. O'Brien, E.T., Kinch, M., Harding, T.W. and Epstein, D.L. (1997) A mechanism for trabecular meshwork cell retraction: ethacrynic acid initiates the dephosphorylation of focal adhesion proteins. *Exp. Eye Res.*, **65**, 471–483.
53. Li, H., Raghunathan, V., Stamer, W.D., Ganapathy, P.S. and Herberg, S. (2022) Extracellular matrix stiffness and TGFbeta2 regulate YAP/TAZ activity in human trabecular meshwork cells. *Front. Cell Dev. Biol.*, **10**, 844342.
54. Liu, Z., Li, S., Qian, X., Li, L., Zhang, H. and Liu, Z. (2021) RhoA/ROCK-YAP/TAZ Axis regulates the fibrotic activity in dexamethasone-treated human trabecular meshwork cells. *Front. Mol. Biosci.*, **8**, 728932.
55. Maddala, R., Skiba, N.P. and Rao, P.V. (2017) Vertebrate lonesome kinase regulated extracellular matrix protein phosphorylation, cell shape, and adhesion in trabecular meshwork cells. *J. Cell. Physiol.*, **232**, 2447–2460.
56. Das, M., Ithychanda, S., Qin, J. and Plow, E.F. (2014) Mechanisms of Talin-dependent integrin signaling and crosstalk. *Biochim. Biophys. Acta*, **1838**, 579–588.
57. Faralli, J.A., Newman, J.R., Sheibani, N., Dedhar, S. and Peters, D.M. (2011) Integrin-linked kinase regulates integrin signaling in human trabecular meshwork cells. *Invest. Ophthalmol. Vis. Sci.*, **52**, 1684–1692.
58. Izard, T. and Brown, D.T. (2016) Mechanisms and functions of vinculin interactions with phospholipids at cell adhesion sites. *J. Biol. Chem.*, **291**, 2548–2555.
59. Cai, X., Yang, Y., Chen, P., Ye, Y., Liu, X., Wu, K. and Yu, M. (2016) Tetramethylpyrazine attenuates Transdifferentiation of TGF-beta2-treated human Tenon's fibroblasts. *Invest. Ophthalmol. Vis. Sci.*, **57**, 4740–4748.
60. Raghunathan, V.K., Morgan, J.T., Chang, Y.R., Weber, D., Phinney, B., Murphy, C.J. and Russell, P. (2015) Transforming growth factor Beta 3 modifies mechanics and composition of extracellular matrix deposited by human trabecular meshwork cells. *ACS Biomater. Sci. Eng.*, **1**, 110–118.
61. Raghunathan, V.K., Morgan, J.T., Park, S.A., Weber, D., Phinney, B.S., Murphy, C.J. and Russell, P. (2015) Dexamethasone stiffens trabecular meshwork, trabecular meshwork cells, and matrix. *Invest. Ophthalmol. Vis. Sci.*, **56**, 4447–4459.
62. Dismuke, W.M., Liang, J., Overby, D.R. and Stamer, W.D. (2014) Concentration-related effects of nitric oxide and endothelin-1 on human trabecular meshwork cell contractility. *Exp. Eye Res.*, **120**, 28–35.
63. Overby, D.R., Zhou, E.H., Vargas-Pinto, R., Pedrigi, R.M., Fuchshofer, R., Braakman, S.T., Gupta, R., Perkumas, K.M., Sherwood, J.M., Vahabikashi, A. *et al.* (2014) Altered mechanobiology of Schlemm's canal endothelial cells in glaucoma. *Proc. Natl. Acad. Sci. U. S. A.*, **111**, 13876–13881.
64. Okamoto, M., Nagahara, M., Tajiri, T., Nakamura, N., Fukunishi, N. and Nagahara, K. (2020) Rho-associated protein kinase inhibitor induced morphological changes in type VI collagen in the human trabecular meshwork. *Br. J. Ophthalmol.*, **104**, 392–397.
65. Honjo, M., Tanihara, H., Inatani, M., Kido, N., Sawamura, T., Yue, B.Y., Narumiya, S. and Honda, Y. (2001) Effects of rho-associated protein kinase inhibitor Y-27632 on intraocular pressure and outflow facility. *Invest. Ophthalmol. Vis. Sci.*, **42**, 137–144.
66. Kaneko, Y., Ohta, M., Inoue, T., Mizuno, K., Isobe, T., Tanabe, S. and Tanihara, H. (2016) Effects of K-115 (Ripasudil), a novel ROCK inhibitor, on trabecular meshwork and Schlemm's canal endothelial cells. *Sci. Rep.*, **6**, 19640.
67. Fujimoto, T., Inoue, T., Kameda, T., Kasaoka, N., Inoue-Mochita, M., Tsuboi, N. and Tanihara, H. (2012) Involvement of RhoA/rho-associated kinase signal transduction pathway in dexamethasone-induced alterations in aqueous outflow. *Investigative Ophthalmology and Visual Sciences*, **53**, 7097–7108.
68. Kameda, T., Inoue, T., Inatani, M., Fujimoto, T., Honjo, M., Kasaoka, N., Inoue-Mochita, M., Yoshimura, N. and Tanihara, H. (2012) The effect of rho-associated protein kinase inhibitor on monkey Schlemm's canal endothelial cells. *Invest. Ophthalmol. Vis. Sci.*, **53**, 3092–3103.
69. Stamer, W.D., Seftor, R.E., Williams, S.K., Samaha, H.A. and Snyder, R.W. (1995) Isolation and culture of human trabecular meshwork cells by extracellular matrix digestion. *Curr. Eye Res.*, **14**, 611–617.
70. Keller, K.E., Bhattacharya, S.K., Borras, T., Brunner, T.M., Chansangpetch, S., Clark, A.F., Dismuke, W.M., Du, Y., Elliott, M.H., Ethier, C.R. *et al.* (2018) Consensus recommendations for trabecular meshwork cell isolation, characterization and culture. *Exp. Eye Res.*, **171**, 164–173.
71. Stamer, W.D., Roberts, B.C., Howell, D.N. and Epstein, D.L. (1998) Isolation, culture, and characterization of endothelial cells from Schlemm's canal. *Invest. Ophthalmol. Vis. Sci.*, **39**, 1804–1812.
72. Perkumas, K.M. and Stamer, W.D. (2012) Protein markers and differentiation in culture for Schlemm's canal endothelial cells. *Exp. Eye Res.*, **96**, 82–87.
73. Patro, R., Duggal, G., Love, M.I., Irizarry, R.A. and Kingsford, C. (2017) Salmon provides fast and bias-aware quantification of transcript expression. *Nat. Methods*, **14**, 417–419.
74. Love, M.I., Huber, W. and Anders, S. (2014) Moderated estimation of fold change and dispersion for RNA-seq data with DESeq2. *Genome Biol.*, **15**, 550.